

Upper critical field peculiarities of superconducting $\text{YNi}_2\text{B}_2\text{C}$ and $\text{LuNi}_2\text{B}_2\text{C}$

S.V. Shulga*, S.-L. Drechsler⁺, G. Fuchs, and K.-H. Müller

Institut für Festkörper- und Werkstofforschung Dresden e.V., Postfach 270016, D-01171 Dresden, Germany

K. Winzer, M. Heinecke, and K. Krug

1. Physikalisches Institut, Universität Göttingen, Bunsenstrasse 9, D-37073 Göttingen, Germany

(7 October 1997)

We present new upper critical field $H_{c2}(T)$ data in a broad temperature region $0.3\text{K} \leq T \leq T_c$ for $\text{LuNi}_2\text{B}_2\text{C}$ and $\text{YNi}_2\text{B}_2\text{C}$ single crystals with well characterized low impurity scattering rates. The absolute values for all T , in particular $H_{c2}(0)$, and the sizeable positive curvature (PC) of $H_{c2}(T)$ at high and intermediate T are explained quantitatively within an effective two-band model. The failure of the isotropic single band approach is discussed in detail. Supported by de Haas van Alphen data, the superconductivity reveals direct insight into details of the electronic structure. The observed maximal PC near T_c gives strong evidence for clean limit type II superconductors.

74.60.Ec, 74.70.Ad, 74.20.-z, 74.72.Ny

The discovery [1,2] of superconductivity in transition metal borocarbides has generated large interest due to their relatively high transition temperatures $T_c \sim 15$ to 23 K and due to the relation between the mechanisms of superconductivity in these compounds, in cuprates, and in ordinary transition metals. Another highlight is the coexistence of magnetism and superconductivity in some of these compounds containing rare earth elements [3–5]. A study of the non-magnetic compounds such as $\text{LNi}_2\text{B}_2\text{C}$, with $L=\text{Lu}, \text{Y}, \text{Th}, \text{Sc}$ [6], is a prerequisite for the understanding of their magnetic counterparts. Experimental data for $\text{LuNi}_2\text{B}_2\text{C}$ [7] demonstrate beside a maximal positive curvature (PC) of $H_{c2}(T)$ near T_c , observed also for $\text{YNi}_2\text{B}_2\text{C}$ [8,4,9], a weak T -dependent anisotropy within the tetragonal basal plane and a T -independent out-of-plane anisotropy of the upper critical field H_{c2} . Both anisotropies have been described [7] in terms of nonlocal corrections to the Ginzburg-Landau (GL) equations. In this picture the PC of $H_{c2}^c(\vec{H} \parallel \text{to the tetragonal c-axis})$ is caused, almost purely, by the basal plane anisotropy. However, it should be noted that the reported anisotropy of H_{c2} for $\text{YNi}_2\text{B}_2\text{C}$ is significantly smaller than for $\text{LuNi}_2\text{B}_2\text{C}$ [7,9,10] whereas its PC is comparable or even larger. Further explanations of the unusual PC of $H_{c2}(T)$, such as quasi-2D fluctuations [11], are excluded by the underestimation of $H_{c2}(T)$ at low- T [9] and the observed weak anisotropy. The quantum critical point scenario [12] as well as the bipolaronic one [13] can be disregarded because the slope of $H_{c2}(T)$ decreases for $T \rightarrow 0$ (see Fig. 1). Local density approximation (LDA) band structure calculations [14,15] predict a nearly isotropic electronic structure with rather complicated bands near the Fermi level E_F . However, in analyzing the superconductivity in terms of an isotropic *single-band* (ISB) Eliashberg model, the multi-band character and the anisotropic Fermi surface have been widely ignored so far.

Here we present and analyze theoretically new data of $H_{c2}(T)$ in a broad interval $0.3\text{K} \leq T \leq T_c$ for high purity

$\text{LuNi}_2\text{B}_2\text{C}$ and $\text{YNi}_2\text{B}_2\text{C}$ single crystals. We show that typical features of both compounds, such as $H_{c2}(0) \sim 8$ to 10 T and the unusual PC of $H_{c2}(T)$ for $T \gtrsim 0.5T_c$, cannot in any way be explained consistently with the normal state properties within the ISB approach. Instead we propose a two-band model (TBM) approach. To clarify its relationship to the extended saddle-point model [16] which also predicts a PC is beyond the scope of our letter.

Platelet shaped $\text{LuNi}_2\text{B}_2\text{C}$ and $\text{YNi}_2\text{B}_2\text{C}$ single crystals with a mass of ~ 1 mg were grown by a high-temperature flux technique with Ni_2B as flux. The values of T_c , 16.5 K and 15.7 K, have been determined by low-

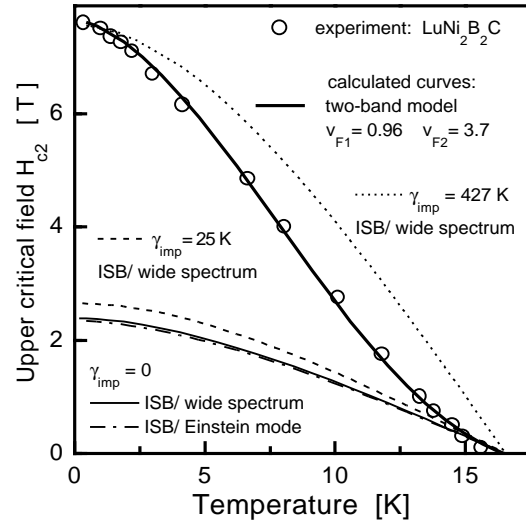


FIG. 1. Experimental data for $H_{c2}(T)$ of $\text{LuNi}_2\text{B}_2\text{C}$ (magnetic field $\vec{H} \parallel \text{the c-axis}$) compared with theoretical curves: (i) the isotropic single band (ISB) model with Fermi velocity $v_F = 2.76 \cdot 10^7$ cm/s and various impurity scattering rates γ_{imp} explained in the text and the legends and (ii) the two-band model (TBM) with v_{Fi} ($i=1,2$) in units of 10^7 cm/s.

field ac susceptibility $\chi(T)$ with transition widths $\Delta T_c = 0.2$ K. The upper critical field $H_{c2}^c(T)$ along the c -axis, shown in Figs. 1 and 2, has been measured resistively for fixed T adopting the midpoint criterion: $\rho(H_{c2}, T) = 0.5\rho(H=0, T=17\text{K}) \equiv 0.5\rho_n$. The transition width $\Delta H = [H(\rho=0.9\rho_n) - H(\rho=0.1\rho_n)]$ increases up to 0.75 T (1.5 T for $\text{LuNi}_2\text{B}_2\text{C}$) at $T < 0.5$ K starting from a nearly constant value of 0.3 T at $T > 4$ K (8 K for $\text{LuNi}_2\text{B}_2\text{C}$). The low residual resistivity $\rho(0) \approx \rho_n = 2.5\mu\Omega\text{cm}$ and the ratio $\rho(300\text{K})/\rho_n = 43$ (27 for $\text{LuNi}_2\text{B}_2\text{C}$), together with the observations of magnetoquantum oscillations [17–19] indicate a high quality and a low impurity content of our samples. This suggests that we are in the clean limit in terms of the traditional theory of type II superconductors [20]. In this limit one has to consider the electronic structure in more detail. We restrict ourselves to an effective two-band model [21] which, especially on the simple BCS-level, has a long history [22]. Due to the neglect of strong coupling effects, a BCS-like theory is not expected to describe real superconductors quantitatively. Such effects must be studied within the Eliashberg theory [23–27]. To calculate H_{c2} we have solved numerically the corresponding linearized equations of Ref. 23,

$$\tilde{\omega}_i(n) = \omega_n + \pi T \sum_{j,m} [\lambda_{i,j}(m-n) + \delta_{mn}(\gamma_{imp;i,j} + \gamma_{imp;i,j}^s)/2\pi T] \text{sgn}(\omega_m), \quad (1)$$

$$\tilde{\Delta}_i(n) = \pi T \sum_{j,m} [\lambda_{i,j}(m-n) - \mu^* \delta_{ij} \theta(\omega_c - |\omega_m|) + \delta_{mn}(\gamma_{imp;i,j} - \gamma_{imp;i,j}^s)/2\pi T] \chi_j(m) \tilde{\Delta}_j(m), \quad (2)$$

$$\chi(n) = (2/\sqrt{\beta_i}) \int_0^\infty dq \exp(-q^2) \times \tan^{-1}(q\sqrt{\beta_i}/(|\tilde{\omega}_i(n)| + i\mu_B H_{c2} \text{sgn}(\omega_n))), \quad (3)$$

$$\beta_i = eH_{c2}v_{Fi}^2/2, \quad (4)$$

$$\lambda_{i,j}(n) = \int_0^\infty d\omega \omega \alpha_{i,j}^2 F(\omega)/(\omega^2 + \omega_n^2). \quad (5)$$

The bands at E_F are labeled by i, j . Here $\omega_n = 2\pi T(2n+1)$ are the Matsubara frequencies, $\alpha_i^2 F(\omega)$ and $\tilde{\Delta}_i$, denote the spectral density, the superconducting order parameter of the i^{th} band respectively. In our approach, as in any two-band model, two gaps, below and above the BCS-value of $3.5k_B T_c$, occur naturally. In general, interband coupling ($i \neq j$) mediated by phonons ($\alpha_{i,j}^2 F(\omega)$) and impurities is important. Since there is no experimental evidence [28,29] for the presence of magnetic impurities in high quality samples, we neglect the magnetic scattering rate γ_{imp}^s . For the quantification of the non-magnetic counterpart $\gamma_{imp} \approx 2\pi T_D$, the Dingle temperatures, T_D , measured by the de Haas-van Alphen (dHvA) effect are very suitable [17–19]. The experimental values $T_D = 2.8$ K and 4K reveal $\gamma_{imp} = 18\text{K}$ and 25K for our $\text{YNi}_2\text{B}_2\text{C}$ and $\text{LuNi}_2\text{B}_2\text{C}$ single crystals, respectively, indicating that the clean limit is reached since

$\gamma_{imp} \leq 2\Delta_0 \approx 51\text{K}$ holds for both samples, where $2\Delta_0$ denotes the smaller of the two gaps. Hence, the scattering by impurities can be neglected setting $\gamma_{imp} = 0$. In the weak coupling limit of an ISB case, Eqs. (1-5) are equivalent to the well-known WHH-theory [30]. Any anisotropy of H_{c2} can be described by a similar, but much more tedious, system of equations [26]. Since the measured anisotropy is relatively weak, it will be ignored for the sake of simplicity. Therefore, only $H_{c2}^c(T)$'s will be compared with those computed for our isotropic models.

The standard ISB model [27] describes *quantitatively* the renormalization of the physical properties of metals due to electron-phonon (el-ph) interaction. The input parameters of the ISB model are the density of states at E_F , $N(0)$, the Fermi velocity v_F , the impurity scattering rate γ_{imp} , the Coulomb pseudopotential μ^* , and the spectral function $\alpha^2 F(\omega)$ of the el-ph interaction. These quantities can be determined from a few experimental data: the normal state low- T electronic specific heat $\gamma_S T$, the plasma frequency ω_{pl} inferred from the optical conductivity, $H_{c2}(0)$, T_c and its isotope exponent α , as well as the normal state low- T dc resistivity $\rho(0) \approx \rho(T_c)$ which similarly to T_D , gives a direct measure of the sample purity. We adopt for the Coulomb pseudopotential $\mu^* = 0.1$ and $\hbar\omega_c = 600$ meV for the energy cutoff in Eq. (2). The total el-ph coupling constant, $\lambda = 2 \int d\omega \alpha^2 F(\omega)/\omega$, can be estimated from the boron isotope effect $\alpha_B \approx 0.2$ [31] and the well-resolved phonon spectrum [32].

We first consider $\text{LuNi}_2\text{B}_2\text{C}$. To find a lower bound for λ , we accounted for only the high-energy carbon phonons centered at 50 meV and the boron branch at 100 meV. Fitting the experimental α_B and T_c values, we obtained the partial coupling constants $\lambda_{100} = 0.31$, $\lambda_{50} = 0.22$, and $\lambda = \lambda_{100} + \lambda_{50} = 0.53$, where the subscripts denote the corresponding phonon energies in meV. An upper bound of $\lambda = 0.77$ has been found using the Lu phonons centered near 9 meV ($\lambda_9 = 0.34$) and the same B band ($\lambda_{100} = 0.43$) as in the case before. In the following a wide averaged spectrum with $\lambda = 0.65$ ($\lambda_{100} = 0.37$, $\lambda_{50} = 0.12$, $\lambda_9 = 0.16$) will be used which reproduces the experimental values of α_B and T_c . $N(0) = 11.8$ mJ/mol $k_B^2 \text{K}^2$ has been estimated from the experimental value [8] of $\gamma_S = 2\pi^2 k_B^2 (1 + \lambda)N(0)/3 = 19.5$ mJ/mol K^2 . The value of $v_F = 2.76 \cdot 10^7$ cm/s follows from the experimental value [33] of the plasma frequency $\hbar\omega_{pl} = \sqrt{4\pi e^2 v_F^2 N(0)/3} = 4.0$ eV. The analogous values for $\text{YNi}_2\text{B}_2\text{C}$ are $\lambda = 0.637$, $N(0) = 11.1$ mJ/mol $k_B^2 \text{K}^2$, $v_F = 3 \cdot 10^7$ cm/s and $H_{c2}(0) = 2\text{T}$, where the data of Refs. 8 and 34 have been used.

We solved Eqs. (1-5) with these parameter sets for two types of spectral densities $\alpha^2 F(\omega)$: (i) a wide averaged spectrum and (ii) a single Einstein mode peaked at $\hbar\omega_E = 42.4$ meV chosen to yield the experimental $T_c = 16.5$ K for $\text{LuNi}_2\text{B}_2\text{C}$ using the same value of $\lambda = 0.65$ as in the first case. The results are shown in Fig.1. Note that in the intermediate coupling regime under consideration, as expected, $H_{c2}(T)$ is insensitive to details of the shape of $\alpha^2 F(\omega)$ [27] and, in the clean-limit case, also insen-

sitive to the actual value of the small scattering rates. Comparing the $\text{LuNi}_2\text{B}_2\text{C}$ data with the ISB curves one clearly realizes strong deviations. In particular, there is a discrepancy of about 3 between experimental and ISB model values of $H_{c2}(0)$. For $\text{YNi}_2\text{B}_2\text{C}$ the discrepancy reaches even a factor of 5. Therefore it makes no sense to discuss any details of the shape of $H_{c2}(T)$, such as the PC, resulting in deviations of the $H_{c2}(T)$ curves of the order 10 to 20 %, until the reason for the large failure to account for the magnitude of $H_{c2}(0)$ has been elucidated. We remind the reader how this serious difficulty was circumvented in previous studies. At first, frequently the quantity $h_{c2}(T) = -H_{c2}(T)/[T_c(dH_{c2}/dT)_{T=T_c}]$, describing the shape of the $H_{c2}(T)$ curve, has been considered, but the *absolute* values of $H_{c2}(T)$ have not been discussed at all [7]. At second, since within the ISB-model $H_{c2}(0)$ is a monotonically *increasing* function of the impurity content, in principle, large $H_{c2}(0)$ -values might be obtained. To check this approach [9] we calculated the impurity scattering rate γ_{imp} which is required to increase $H_{c2}(0)$ up to the $\text{LuNi}_2\text{B}_2\text{C}$ value of 7.6 T. Thus we obtain $\gamma_{imp} \approx 427$ K which would lead to $\rho(0) \approx 17 \mu\Omega\text{cm}$ which strongly deviates from the experimental value $\rho(0) \approx 2.5 \mu\Omega\text{cm}$. In this context we note that our data and those of Ref. 35 show dependencies just opposite to those predicted by the ISB-model: $H_{c2}(0)$ and T_c *increase* when γ_{imp} decreases! At third, a further empirical parameter, the clean limit coherence length, has been introduced in Ref. 35. However, this results in the overdetermination of the model parameter set and the consistency of the two values v_F obtained using (i) a clean-limit coherence length and (ii) normal state data has not been checked. Thus the ISB approach fails to explain simultaneously the three values $\gamma_S=19.5$ mJ/mol K², $\hbar\omega_{pl}=4$ eV, $H_{c2}(0)=7.6$ T in the clean limit, and the four values γ_S , ω_{pl} , $H_{c2}(0)$, $\rho=2.5 \mu\Omega\text{cm}$ in the dirty limit. In addition, the ISB model is also unable to explain the small gap values $2\Delta_0/k_B T_c < 3.5$ observed in microwave [36], tunneling [10], and dHvA [37] measurements. Furthermore the PC of $H_{c2}(T)$ near T_c and the extended quasi-linear behavior of $H_{c2}(T)$ down to $T \sim 1$ to 2 K cannot be described within the ISB. The ISB model with a *single* v_F contradicts the dHvA data which clearly show the presence of at least six different sections F_α, \dots, F_η [18,19] with roughly *two* or *three* groups of v_F 's.

Turning to our TBM we solved Eqs. (1-5). For the sake of simplicity, the same phonon spectrum as in the ISB case discussed above has been adopted. We achieve an excellent agreement with the $\text{LuNi}_2\text{B}_2\text{C}$ data (see Fig. 1) for $\lambda_1=0.51$, $\lambda_2=\lambda_{21}=0.2$, $\lambda_{12}=0.4$, $\mu_1^*=\mu_2^*=0.1$, $v_{F2}=3.7 \cdot 10^7$ cm/s, $v_{F1}=0.96 \cdot 10^7$ cm/s. For $\text{YNi}_2\text{B}_2\text{C}$ we used the following set: $\lambda_1=0.5$, $\lambda_2=\lambda_{21}=0.2$, $\lambda_{12}=0.4$, $\mu_1^*=\mu_2^*=0.1$, $v_{F2}=3.8 \cdot 10^7$ cm/s, $v_{F1}=0.85 \cdot 10^7$ cm/s, $N(0)=11$ mJ/mol k_B^2 K². Reproducing $T_c=15.6$ K, the adopted values of $N(0)$ agrees well with the LDA-value [15] of 9.5 mJ/mol k_B^2 K². The plasma frequency $\hbar\omega_{pl}=4.4$ eV is in accord with $\hbar\omega_{pl}=4.25$ eV obtained in Ref. 34. From the ob-

tained v_F 's it is concluded that ω_{pl} is mainly related to the second weakly coupled band. Then transport, optical and tunneling data mainly exhibit the properties of that band whereas the strongly coupled band remains almost hidden. The calculated value of the penetration depth at 4.2 K, 100 nm, is in agreement with the data of Ref. 35. Our $\gamma_S=17.2$ mJ/mol K² should be compared with $\gamma_S=18.2$ mJ/mol K² reported in Ref. 8. Finally, we arrive at $H_{c2}(0)=9.4$ to 9.9 T in good agreement with our experimental value $H_{c2}(0)=10.6 \pm 0.2$ T. The experimental $H_{c2}(T)$ curve of $\text{YNi}_2\text{B}_2\text{C}$ together with results of the TBM are shown in Fig. 2. The values $v_F \approx 4.2 \cdot 10^7$ cm/s and 0.7 to $1.3 \cdot 10^7$ cm/s of the extremal orbits F_β and $F_{\eta 1/2}$, respectively, derived from earlier dHvA data [18,19] on the same $\text{YNi}_2\text{B}_2\text{C}$ single crystal do not deviate much from the parameters $v_{F2} \approx 3.8 \cdot 10^7$ cm/s and $v_{F1} \approx 0.8$ to $0.96 \cdot 10^7$ cm/s introduced empirically in our approach. The remaining deviations might be due to natural differences between v_F 's on extremal orbits seen in the dHvA-experiments and the corresponding *effective* quantities of our TBM which contains implicitly information on the whole Fermi surface.

Further calculations within our TBM reveal that the PC of $H_{c2}(T)$ mainly depends upon the strength of the interband coupling ($\lambda_{12}, \lambda_{21}$) and to a lesser extent upon the ratio of the Fermi velocities and the intraband coupling strength (λ_1, λ_2). These findings may also be interpreted in terms of the flat Ni-derived band near E_F and the dispersive bands crossing E_F seen in the LDA-band structure [14]. The strong mixing of these bands might be viewed as the microscopic origin for significant interband coupling. Further work is required to clarify this point. For low $T < 4$ K, $H_{c2}(T)$ is very sensitive to the

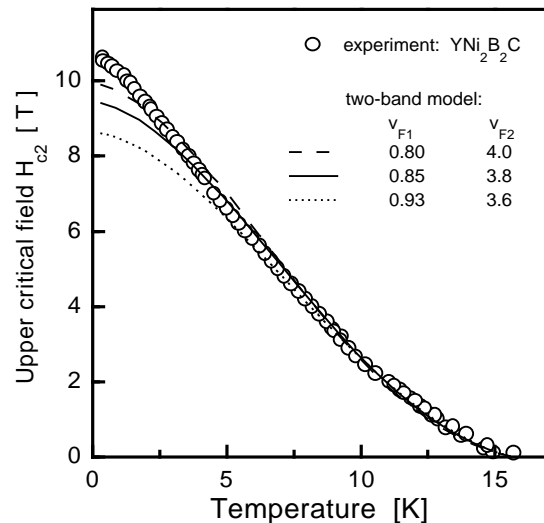


FIG. 2. Temperature dependence of $H_{c2}(T)$ for $\text{YNi}_2\text{B}_2\text{C}$. Experimental points for the magnetic field $\vec{H} \parallel c$ -axis. The Fermi-velocities of the two-band model (TBM) are given in units of 10^7 cm/s. For the interaction constants see the text.

actual $v_{F,2}/v_{F,1}$ ratio. This is illustrated by the additional curves shown in Fig. 2. The variation of v_{F1} and v_{F2} results in slightly higher and lower $H_{c2}(0)$ values, respectively. Our empirical parameter sets for $\text{LuNi}_2\text{B}_2\text{C}$ and $\text{YNi}_2\text{B}_2\text{C}$ differ almost only in their v_{F1} values which roughly scale with the Ni-Ni distance as $d_{\text{Ni-Ni}}^{-5}$. In this context the study of $\text{Sc(Th)Ni}_2\text{B}_2\text{C}$ crystals having much reduced (increased) Ni-Ni distances is of interest.

Our analysis reveals that both compounds can be well described within an effective two-band model provided there are at least two groups of electrons having (i) significantly different Fermi-velocities, (ii) strong coupling in the small- v_F band, as well as (iii) sizeable coupling between the small- v_F and the large- v_F band. This case differs from the situation considered in Refs. 24 and 26. There, the stronger coupling is in the large- v_F band and the curvature of $H_{c2}(T)$ near T_c is *negative*. A PC would only appear at intermediate T if the interband coupling and the impurity scattering are both weak. In contrast, in this region $H_{c2}(T)$ shows almost no curvature in our model. In other words, the result of Refs. 24 and 26 can be understood as an average over two weakly coupled superconductors, the first with a high $H_{c2}(0)$ but a low T_c and the second one with a small $H_{c2}(0)$ but high T_c . In our case the isolated small- v_F subsystem would have high values of λ , $H_{c2}(0)$, and T_c . The values of $H_{c2}(0)$ and T_c of the coupled system are reduced by the second large- v_F subsystem with weak interaction parameters. In this case, which to the best of our knowledge has not been considered so far, the PC of the resulting $H_{c2}(T)$ near T_c becomes a direct manifestation of that interband coupling. In our TBM, the PC of $H_{c2}(T)$, as well as $H_{c2}(0)$, and T_c are suppressed by growing impurity content and the PC vanishes upon reaching the dirty limit with $T_c \approx 11$ K. Thus the observed maximal PC of $H_{c2}(T)$ near T_c of multi-band systems of the type under consideration can be regarded as a direct measure of the high sample quality, as opposed to the widely spread belief attributing it simply to sample inhomogeneities. The latter scenario is excluded by the sharp transition in the $\chi(T)$ data.

To summarize, we have shown that the superconductivity of pure non-magnetic borocarbides should be described within a multi-band picture. The isotropic TBM gives a reasonable starting point toward the understanding of the mechanism of superconductivity in these compounds. Combined studies of quantum oscillations (dHvA) and $H_{c2}(T)$ unified by Eliashberg analysis are found to be valuable supplementary tools to elucidate the specific role of subgroups of electrons having small v_F 's and strong coupling to bosons. These electrons may be readily overlooked by other experimental techniques.

We thank O. Dolgov, D. Rainer, E. Maksimov, H. Braun, N. Schopohl, M. Golden, J. Fink, L. Schultz, H. Eschrig, and A. Gladun for discussions. This work was supported by the INTAS-93-2154 grant, the SFB 463, and the Deutsche Forschungsgemeinschaft.

-
- * On leave from Inst. of Spectroscopy RAS, 142092 Troitsk, Russia. E-mail: shulga@fly.triniti.troitsk.ru
+ Corresp. author, E-mail: drechsler@ifw-dresden.de
- [1] R.J. Cava *et al.*, Nature (London) **367**, 146, 252 (1994).
 - [2] R. Nagarajan *et al.*, Phys. Rev. Lett. **72**, 274 (1994).
 - [3] B.K. Cho *et al.*, Phys. Rev. B **52**, R3844 (1995).
 - [4] K. Eversmann, *et al.*, Physica C **266**, 27 (1996).
 - [5] K.-H. Müller *et al.*, J. Appl. Phys. **81**, 4240 (1997).
 - [6] C.C. Lai, *et al.*, Phys. Rev. B **51**, 420 (1995).
 - [7] V. Metlushko *et al.*, Phys. Rev. Lett. **79**, 1738 (1997).
 - [8] H. Michor *et al.*, Phys. Rev. B **52**, 16165 (1995).
 - [9] K.D.D. Rathnayaka *et al.*, Phys. Rev. B **55**, 8506 (1997).
 - [10] Y. De Wilde *et al.*, Phys. Rev. Lett. **78**, 4273 (1997).
 - [11] S.R. Bahcall, Phys. Rev. Lett. **75**, 1376 (1995).
 - [12] G. Kotliar *et al.*, Phys. Rev. Lett. **77**, 2296 (1996).
 - [13] A.S. Alexandrov, Phys. Rev. B **48**, 10571 (1993).
 - [14] W.E. Pickett *et al.*, Phys. Rev. Lett. **72**, 3702 (1994).
 - [15] J.I. Lee *et al.*, Phys. Rev. B **50**, 4030 (1994).
 - [16] A.A. Abrikosov, Phys. Rev. B **56**, 5112 (1997).
 - [17] M. Heinecke and K. Winzer, Z. Phys. B **98**, 147 (1995).
 - [18] G. Goll *et al.*, Phys. Rev. B **53**, R8871 (1996).
 - [19] L.H. Nguyen *et al.*, J. Low Temp. Phys. **105**, 1653 (1996).
 - [20] Using the most complete dHvA data available for $\text{YNi}_2\text{B}_2\text{C}$, only, the mean free path $l_q = \hbar v_F / 2\pi k_B T_D$ for electrons belonging to different cross sections can be estimated as 181, 86, 56, and 30 nm, where the Fermi velocities v_F of 4.2, 2, 1.3, and $0.7 \cdot 10^7$ cm/s, respectively, and the Dingle temperature $T_D = 2.8$ K have been used. From $\rho(0) \approx \rho_n = 2.5 \mu\Omega\text{cm}$, $l_\rho = 4\pi v_F / \omega_{pl}^2 \rho(0)$ only the mean free paths of the large v_F bands can be estimated as $l_\rho \approx 41$ (45), where $\omega_{pl} = 4.25$ (4.0) eV and $v_F = 3.6$ (3.7) $\cdot 10^7$ cm/s have been used. All estimated l 's exceed significantly the GL-coherence length $\xi_0 = \sqrt{\Phi_0 / 2\pi H_{c2}(0)} = 5.5$ (6.5) nm for $\text{YNi}_2\text{B}_2\text{C}$ ($\text{LuNi}_2\text{B}_2\text{C}$).
 - [21] Note that the term "two-band" should not be taken too literally. Within the Eliashberg theory [23–26] a single anisotropic band model is equivalent to an isotropic multi-band model more suitable for theoretical studies.
 - [22] H. Suhl *et al.*, Phys. Rev. Lett. **3**, 552, (1959).
 - [23] M. Prohammer *et al.*, Phys. Rev. B **36**, 8353 (1987).
 - [24] P. Entel *et al.*, J. of Low Temp. Phys. **22**, 613 (1976).
 - [25] P.B. Allen, Phys. Rev. B **13**, 1416 (1976).
 - [26] E. Langmann, Phys. Rev. B **46**, 9104 (1992).
 - [27] J.P. Carbotte, Rev. Mod. Phys. **62**, 1027 (1990).
 - [28] H. Schmidt *et al.*, Physica C **235-240**, 779 (1994).
 - [29] B.J. Suh *et al.*, Phys. Rev. B. **53** R6022 (1996).
 - [30] N.R. Werthamer *et al.*, Phys. Rev. **147**, 295 (1966).
 - [31] D.D. Lawrie *et al.*, Physica C **245**, 159 (1995).
 - [32] F. Gompf *et al.*, Phys. Rev. B **55**, 9058 (1997).
 - [33] F. Bommeli *et al.*, Phys. Rev. Lett. **78**, 547 (1997).
 - [34] K. Widder *et al.*, Europhys. Lett. **30**, 55 (1995).
 - [35] H. Schmidt *et al.*, Phys. Rev. B **55**, 8497 (1997).
 - [36] T. Jacobs *et al.*, Phys. Rev. B **52**, R7022 (1995).
 - [37] T. Terashima *et al.*, Phys. Rev. B **56**, 5120 (1997).